New diagnostic method for Alzheimer's disease based on the toxic conformation theory of amyloid β

Kazuhiro Irie

Division of Food Science and Biotechnology, Graduate School of Agriculture, Kyoto University, Kyoto 606-8502, Japan

CONTACT Kazuhiro Irie: irie@kais.kyoto-u.ac.jp

This review was written in response to the author's receipt of the Japan Society for Bioscience, Biotechnology, and Agrochemistry Award in 2019.

Abstract

Recent investigations suggest that soluble oligomeric amyloid β (Aβ) species may be involved in early onset of Alzheimer's disease (AD). Using systematic proline replacement, solid-state NMR, and ESR, we identified a toxic turn at position 22 and 23 of Aβ42, the most potent neurotoxic Aβ species. Through radicalization, the toxic turn can induce formation of the C-terminal hydrophobic core to obtain putative Aβ42 dimers and trimers. Synthesized dimer and trimer models showed that the C-terminal hydrophobic core plays a critical role in formation of high molecular weight oligomers with neurotoxicity. Accordingly, an anti-toxic turn antibody (24B3) that selectively recognizes a toxic dimer model of E22P-Aβ42 was developed. Sandwich enzyme-linked immunosorbent assay with 24B3 and 82E1 detected a significantly higher ratio of Aβ42 with a toxic turn to total Aβ42 in cerebrospinal fluid of AD patients compared with controls, suggesting that 24B3 could be useful for early onset of AD diagnosis.

Keywords: Alzheimer's disease; amyloid β; antibody; protein kinase C; solid-phase peptide synthesis

The opportunity to start this research

First, I would like to explain the background to this study. My first original paper [1] was on the isolation and Epstein–Barr virus-inducing activity of (–)-indolactam-V (IL-V) [2], the basic ring structure of teleocidins [3-5], from *Streptomyces blastmyceticum*. IL-V is a tumor promoter and activator of protein kinase C (PKC) isozymes [6,7], the key enzyme family involved in signal transduction on the cell surface [8]. Since *Streptomyces blastmyceticum* produces a large amount of IL-V, detailed structure–activity relationship studies were performed to clarify the structural requirements of its tumor-promoting activity [9,10]. Consequently, the next step was to identify the binding mode of IL-V with PKC isozymes, whose binding sites are two C1 domains: C1A and C1B [11-13]. For this purpose, it was necessary to prepare PKC isozymes in sufficient quantity. However, there were difficulties in obtaining PKC isozymes with potent binding affinity to various PKC ligands; namely, phorbol 12,13-dibutyrate (PDBu), IL-V, and teleocidins. Specifically, the C1 domains were highly sensitive to oxidation because of their cysteine-rich sequence with a zinc-finger-like structure (ring-finger).

In 1992, I was in Stanford University as a visiting scholar, when Professor Paul A. Wender advised me to synthesize each PKC C1 domain by solid-phase peptide synthesis. Based on his advice, two PKCγ C1 domain peptides (PKCγ-C1A and PKCγ-C1B) of approximately 50 amino acid residues were custom synthesized at Stanford University. Fortunately, we detected weak but significant [^{3}H]PDBu binding against each of them, although their purity and binding constants (K_d) were not satisfactory [14]. After returning home in 1993, I started to establish a synthetic method of long peptides without fragment condensation in collaboration with Dr. Hiroyuki Fukuda at Applied Biosystems, Japan. After struggling for five years, we eventually succeeded in synthesizing all PKC isozyme C1 domains at high purity, and were able to precisely determine their K_d values against

[^{3}H]PDBu [15-17]. The representative example (PKCδ-C1B) is shown in Figure 1. This data provided the basis for rational design of new medicinal leads with PKC isozyme selectivity. Moreover, we identified diacylglycerol kinase (DGK) β and γ as new PDBu receptors using synthetic C1 peptides of all DGK isozymes [18]. We were even able to synthesize a 116-mer PKCγ-C1A-C1B peptide without fragment condensation [19]. The core method of this synthesis consists of three points: polyethylene glycol polystyrene support as a resin, hexafluorophosphate azabenzotriazole tetramethyl uronium (HATU) developed by Carpino [20] as a highly efficient activator, and the continuous flow-type peptide synthesizer, Pioneer™ supplied by Applied Biosystems. Unfortunately, this machine has been out of service since 2008, and we have recently introduced a microwave-type peptide synthesizer, Biotage Initiator+ Alstra™ (Biotage). The opportunity to start my research was the establishment of this peptide synthesis technology, and also my encounter with Dr. Fukuda, who collaborated with Dr. Takuji Shirasawa at Tokyo Metropolitan Institute of Gerontology, a world-renowned scientist in amyloid β research.

Toxic conformation theory of amyloid β

Alzheimer's disease (AD) is one of the most common neurodegenerative disorders, characterized by extracellular amyloid fibrils and intracellular neurofibrillary tangles (Figure 2) [21]. The former consist mainly of 40- or 42-mer amyloid β protein (Aβ40 and Aβ42), while the latter are composed of hyperphosphorylated tau protein. AD proceeds along a sequence of aggregation (oligomerization) of Aβ, hyperphosphorylation of tau protein, and ultimately, loss of nerve cells (amyloid hypothesis, Figure 3) [22]. More recently, accumulated evidence suggests that soluble Aβ oligomers, rather than Aβ fibrils, play a more important role in the pathogenesis of AD because of their more potent

neurotoxicity [23-25]. In 1999, when I began my research on Aβ, the molecular mechanism of Aβ aggregation and neurotoxicity had not been determined, and even the secondary structure of the "toxic oligomers" remained unknown. The main reasons for this were because of difficulties in the synthesis of Aβ42, the most toxic and highly aggregative species, and its highly aggregative character, making high-resolution X-ray crystallography and liquid-phase nuclear magnetic resonance (NMR) analysis almost impossible. Although solid-phase NMR analysis on aggregates of Aβ40, the less neurotoxic and less aggregative species, were first reported by Tycko's group in 2002 [26], there were few reports on the precise structure of Aβ42 aggregates until 2015 [27-29].

First, a systematic proline replacement approach was adopted to identify the secondary structure of Aβ42 responsible for its potent aggregative ability and neurotoxicity. Prolines are not present in β-sheet structures but are easily accommodated in turn structures. Wood *et al.*, [30] reported the first proline replacement on Aβ fragments (Aβ15–23 and Aβ12–26), and suggested that the residues at position 17–23 are involved in intermolecular β-sheets of Aβ fibrils. However, such replacements should be performed using full-length Aβ42, whose solid-phase synthesis is difficult because of its last 14 C-terminal hydrophobic and bulky amino acid residues. As described, my colleagues and I had developed a practical and efficient method to synthesize hydrophobic and bulky peptides of over 50 amino acid residues without fragment condensation [15], enabling the flexible replacement of each amino acid residue of Aβ42 with proline [31,32].

Approximately 40 proline-substituted mutants of Aβ42 were synthesized to examine their aggregative velocity, thermodynamic stability of their aggregates, and neurotoxicity against rat phaeochromocytoma (PC12) cells. The resultant data suggested that the

residues at positions 15–21 and 24–32 were involved in the intermolecular β-sheet structure of Aβ42 aggregates, and that the turn at position 22 and 23 plays a critical role in aggregation and neurotoxicity of Aβ42. Notably, mutation sites in familial AD are concentrated at this position [33,34]. Although the N-terminal 13 residues did not adopt any solid structure in Aβ42 aggregates, the C-terminal eight residues participated in their intramolecular β-sheet structure [35]. Based on these findings, we proposed toxic dimer and trimer models, as shown in Figure 4 [36].

Several reports suggested that radicalization of both Tyr10 and Met35 was important for inducing aggregation and neurotoxicity of Aβ42 [37-39]. Radicalization of Tyr10 by coordinated Cu(II) at His residues at positions 6, 13, and 14 of Aβ42 is considered to be an initial event for Aβ42 to aggregate and induce neurotoxicity [40]. Accordingly, Tyr10 could be converted to a phenoxy radical by the reaction of Cu(II) to Cu(I) to obtain hydrogen peroxide. In our model, phenoxy radical can efficiently oxidize Met35 by formation of a turn at position 22 and 23, bringing Tyr10 and Met35 closer together [41,42]. The resultant cation radical of Met35 can be ionically stabilized by the C-terminal carboxylate of Ala42, forming a hydrophobic core that accelerates aggregation to form a dimer and trimer. Since carboxyl radicals are incorporated in aggregates, liberation of these radicals will cause oxidative stress against neuronal cells for extended periods of time. This is our “toxic conformation theory”, and the turn at position 22 and 23 is called a “toxic turn” (Figure 4).

To confirm the presence of the toxic turn, solid-state NMR of partially ^{13}C- and ^{15}N-labeled Aβ42 at positions 21–24 or 25–27 was measured after aggregation using ^{13}C-^{1}H dipolar assisted rotational resonance [43,44], in collaboration with Professor Kiyonori Takegoshi at Kyoto University. The data clearly showed the presence of turns at position 22 and 23 and position 25 and 26 in aggregates of wild-type Aβ42 and E22K-Aβ42

151 (Italian mutation for familial AD [45]) [46,47]. Moreover, conformationally-fixed Aβ42
152 with a lactam ring at position 22 and 23 was neurotoxic, while a lactam ring at position
153 25 and 26 was virtually non-toxic [47]. Aβ42 is produced from amyloid precursor protein
154 (APP) by two secretases [48]. Aβ42 monomer is in equilibrium between two conformers
155 with a turn at positions 22 and 23 or 25 and 26, with the former aggregating to form toxic
156 oligomers (Figure 5).

157 Systematic proline replacement of Aβ40 was also reported by Wetzel's group in
158 2004 [49]. Although the C-terminal structure of Aβ40 is different from Aβ42, the turn at
159 position 22 and 23 was also present in Aβ40 aggregates. The turn mimic peptide, E22P-
160 Aβ40, was more aggregative and neurotoxic compared with wild-type Aβ40, suggesting
161 that the turn at position 22 and 23 in Aβ40 was pathological [31,32]. However, the
162 position of the turn determined by solid-state NMR was different in Aβ40 aggregates [26]
163 (Figure 6). The turn was present near position 25 and 26, which is similar to the nontoxic
164 conformer in Aβ42 aggregates [47], because of the presence of a salt bridge between
165 Asp23 and Lys28.

166 Recently, the structure of highly homogeneous Aβ42 aggregates determined by
167 solid-state NMR was independently reported by three groups [27-29]. Surprisingly, the
168 turn position in Aβ42 aggregates was quite different from that in Aβ40 aggregates: in the
169 former, it was near position 22 and 23, while it was near position 25 and 26 in the latter.
170 Both of these positions correlate with our proposed turn structures in Aβ42 aggregates
171 (Figure 6). The presence of Ile41 and Ala42 at the C-terminus of Aβ42 could create a salt
172 bridge between the primary ammonium ion of Lys28 and carboxylate anion of Ala42 to
173 fix the molecule with a turn at position 22 and 23, unlike Aβ40. This clearly demonstrates

that Aβ42 is more aggregative and neurotoxic than Aβ40 since the turn at position 22 and 23 is important to induce aggregation and neurotoxicity of Aβ.

Synthesis and characterization of dimer models of Aβ

As described, my colleagues and I identified the key structure (toxic turn) of Aβ42 that induces aggregation and neurotoxicity. Recent investigations suggest that Aβ oligomers are more neurotoxic than mature Aβ fibrils [23-25]. However, Aβ oligomers are labile and in complex equilibrium among monomers, several oligomers, and mature fibrils (Figure 7). For example, 12-mers and 24-mers might form from dimers and/or trimers as a minimum unit. Further, some Aβ oligomers are unable to form amyloid fibrils to exist as quasi-stable oligomers (off-pathway), while others directly aggregate into fibrils (on-pathway). It is difficult to separate pure oligomeric species for biological evaluation. To solve this problem, two approaches have been attempted: stabilization of Aβ oligomers by photo-induced cross-linking, and synthesis of chemically pure and stable Aβ oligomer models.

Teplow's group isolated dimers, trimers, and tetramers of Aβ40 using photo-induced cross-linking after incubation, and showed that their neurotoxicity was higher than Aβ40 monomers [50]. However, each oligomeric species might be a complex mixture of compounds with different three-dimensional structures since various positions of cross-linking are possible. It is therefore difficult to determine which three-dimensional structure is responsible for the toxicity observed in neuronal cells. Alternatively, there are several reports on the synthesis of dimer models of Aβ40 [51-55]. Nonetheless, in all cases, toxic conformation of Aβ40 was not considered. Moreover, the linker positions were almost within N-terminal regions rather than C-terminal ones which are involved in

198 the formation of a hydrophobic core to induce oligomerization (Figure 4). Most of these
199 models formed aggregative amyloid fibrils, and some were neurotoxic [52,54,55].
200 Based on our toxic dimer model (Figure 4), three dimer models were synthesized:
201 two with linkers at positions 30 or 38 of Aβ40 (**1**–**3**), and one with a linker at position 40
202 of Aβ42 (**4**) [56,57] (Figure 8). L,L-2,6-Diaminopimeric acid (DAP) or L,L-2,6-
203 diaminoazelaic acid (DAZ) were used as linkers. Although DAP was previously used by
204 Kok *et al.*, [51] for the synthesis of a dimer model with a DAP linker at position 10 to
205 mimic the dityrosine-linked dimer of Aβ40, there have been no reports using DAZ as a
206 linker for Aβ dimers. Since the distance between the two methyl groups of Ala30 in
207 E22K-Aβ42 aggregates was estimated by solid-state NMR to be 5–6 Å [58], the DAZ
208 linker was preferable for simulating the intramolecular β-sheet at position 31–36 of the
209 Aβ40 dimer model. To mimic the toxic turn at position 22 and 23, the E22P-mutant was
210 used.
211 Synthesis of **1**–**4** was started by preparation of optically pure di-Fmoc-L,L-DAP and
212 di-Fmoc-L,L-DAZ. The method of Paradisi *et al.*, [59] was adopted, albeit with slight
213 modifications [56]. Solid-phase synthesis on a continuous flow-type peptide synthesizer
214 (Pioneer™) was performed using di-Fmoc-L,L-DAP or di-Fmoc-L,L-DAZ (0.5
215 equivalent with respect to the loading peptide to avoid formation of a monocoupled
216 peptide), in accordance with Kok's study [51]. The purity of the dimers (**1**–**4**) was > 98%,
217 as determined by high performance liquid chromatography (HPLC) analysis and
218 electrospray ionization-quadrupole time-of-flight-mass spectrometry (ESI-qTOF-MS)
219 measurements. Further, dimer yields were 5.6, 3.1, 11.6, and 6.0%, respectively [56,57].
220 Although dimer **2**, with a DAZ linker, had higher β-sheet content than **1** with a DAP
221 linker as expected, the neurotoxicity of **2** as well as **1** against SH-SY5Y neuroblastoma
222 cell lines was absent, even at 10 μM [56]. In contrast, dimer **3**, with a DAP linker in the

C-terminal hydrophobic core at position 38, exhibited more potent neurotoxicity than the corresponding monomer, E22P-Aβ40. All these dimer models exhibited weak thioflavin-T (Th-T) fluorescence after 48 h incubation, which reflected the amount of Aβ aggregates, suggesting they exist as quasi-stable oligomeric species even after 24–48 h incubation [56].

However, characterization of the Aβ oligomers responsible for AD pathogenesis has been controversial. Conventional techniques such as sodium dodecyl sulfate–polyacrylamide gel electrophoresis (SDS-PAGE) and size-exclusion chromatography (SEC) can be useful for this purpose, but SDS induces Aβ oligomerization [60]. Additionally, SEC cannot accurately determine molecular weight since there are no ideal calibration proteins for Aβ. Recently, ion mobility-mass spectrometry (IM-MS) combined with ESI as a native ionization technique, has enabled separation of various Aβ oligomers to accurately determine their molecular weight without using organic solvents that disrupt noncovalent interactions within Aβ oligomers [61-63]. In fact, 2–12-mer aggregates of Aβ40 and Aβ42 have been assigned by IM-MS. However, larger oligomers could not be detected because of the high aggregative velocity of Aβ monomers.

In collaboration with Dr. Kenji Hirose and Mr. Taiji Kawase at Japan Waters Ltd., IM-MS measurements of **1**–**3** were performed after 4 h incubations [56]. Similar spectra were obtained even after 24 h incubations. The representative two-dimensional heat maps with *m/z* domains and drift times are shown in Figure 9. Dimers **1** and **2**, with a DAP or DAZ linker at position 30, existed predominantly as hexamers in monomer conversion (n = 3), with oligomer distribution of 2–12-mer (n = 1–6). In contrast, dimer **3**, with a DAP linker at position 38, existed as 12–24-mers (n = 6–12). The fact that only **3** exhibited more potent neurotoxicity than E22P-Aβ40 monomer, suggests that hydrophobic interaction of the C-terminal region of Aβ is indispensable for formation of larger toxic

oligomers, and that the oligomer size necessary to induce neurotoxicity is around 20-mer in monomer conversion.

According to our "toxic-conformation theory", formation of the C-terminal hydrophobic core may be the initial event for Aβ42 to induce oligomer formation and exhibit neurotoxicity through radicalization (Figure 4) [36]. Although the C-terminal hydrophobic core could not easily form in Aβ40, a DAP linker at position 38 enabled Aβ40 to form toxic oligomers such as Aβ42. In fact, the corresponding Aβ42 version of **3**, E22P,V40DAP-Aβ42 dimer (**4),** also existed as a 12–24-mer in monomer conversion (n = 6–12) (unpublished results), and was significantly neurotoxic [57]. Dimers **3** and **4** may thus be one of the practical toxic dimer models of Aβ since they form quasi-stable protofibrillar aggregates with potent neurotoxicity, and consequently can be regarded as "off-pathway" aggregates.

Synthesis and characterization of trimer models of Aβ

Aβ oligomers originated from Aβ dimers may be involved in the pathogenesis of AD [64-66]. However, several investigations have suggested involvement of Aβ trimers, which show more potent synapse toxicity such as inhibition of long-term potentiation (LTP) than Aβ dimers or tetramers [67,68]. There were no reports on the synthesis and characterization of full-length Aβ trimer models, although trimer models of Aβ fragments were synthesized [69,70]. As my colleagues and I had experienced previously with systematic proline replacement [31,32], such models should be made for full-length Aβ. There are two possible trimer models: one consists of two intermolecular parallel β-sheets, with an additional Aβ monomer bound to the dimer model, while the other is a propeller-type model, as shown in Figure 4. Recently, this type of trimer was identified by solid-

state NMR in 150 kDa oligomers of Aβ42 [71]. Since the propeller-type model is quite different from the dimer models with intermolecular parallel β-sheets, we attempted to mimic this trimer structure.

After molecular modeling studies, 1,3,5-phenyltris-L-alanine (PtA) was adopted as a trimer linker to reproduce a stable trimer structure (Figure 10A) [72]. Synthesis of tri-Fmoc-PtA was performed based on the approach of Ritzén *et al.* [73]. With asymmetric hydrogenation, Imamoto's Rh-(*S*,*S*)-QuinoxP [74] produced excellent results (> 98%ee, > 98%de). Three trimer models of E22P-Aβ40 with the PtA linker at position 34, 36, or 38 (**5**–**7**) were synthesized on a microwave peptide synthesizer (Initiator+ Alstra™, Biotage) using tri-Fmoc-PtA (0.33 equivalent was used to avoid formation of partially coupled PtA) (Figure 10B). Using C4 and C18 columns, trimer models with E22P mutation of Aβ40 (**5**–**7**) were obtained at yields of 0.58, 1.1, and 0.45% after HPLC purification. Purity was checked by HPLC analysis and molecular formulae confirmed by ESI-qTOF-MS measurements [72]. Unexpectedly, continuous flow-type peptide synthesizer (Pioneer™) without heating and microwave irradiation did not produce these target molecules, possibly because the molecular motion might be strongly restricted by the trimer linker, thereby suppressing coupling reactions by steric hinderance at room temperature.

With the trimer models (**5**–**7**), neurotoxicity against SH-SY5Y cells was far less compared with dimer model **3** and E22P-Aβ40 monomer [72]. Only **7**, with a PtA linker at position 38, exhibited significant but weak neurotoxicity compared with E22P-Aβ40. IM-MS measurements suggested that an oligomer size of **7** was 9–21-mer in monomer conversion (n = 3–7), which is comparable to **3** (12–24-mer). In contrast, oligomer sizes of **5** and **6**, both without neurotoxicity, were 3–6-mer (n = 1–2) and 3–12-mer (n = 1–4), respectively. The 150 kDa oligomer of Aβ42 [71] contained a trimer structure with an

297 anti-parallel β-sheet at the C-terminus. However, the corresponding trimer model **6** did
298 not exhibit any neurotoxicity, even at 10 μM. In general, neurotoxicity of Aβ is
299 considered to be ascribable to the aggregation process, not specific oligomers [75]. Since
300 both **3** and **7** formed amyloid fibrils over 48 h incubation, this suggests that tertiary
301 structure as well as oligomer size can contribute to neurotoxicity. The concentration of
302 oligomers might also be important. Neurotoxicity (cell death) by aggregation at the cell
303 surface requires high oligomer concentration (>1 μM), while synapse toxicity of
304 oligomers was observed at a low concentration (< 1 μM) [24].

305 Hitherto, several correlations between oligomer size and neurotoxicity have been
306 reported [24]. For example, ADDL (3–24-mer) [76] and AβO (15–20-mer) [77] are
307 neurotoxic, while synapse toxicity such as LTP was induced by Aβ*56 (12-mer) [78] and
308 even a dimer or trimer of Aβ. This indicates that the oligomer size necessary for
309 neurotoxicity and synapse toxicity can be quite different. In addition, the presence of
310 larger oligomers, such as protofibrils (36–700-mer) [79] and amylospheroids (~ 150-mer)
311 [80], suggests that specific oligomers alone cannot explain neurotoxicity. Our data
312 suggests that at least Aβ oligomers < 12-mer are not neurotoxic. Synapse toxicity of the
313 trimer models is thus worth investigating. However, caution should be applied since
314 synthetic oligomers do not always reflect the heterogeneous Aβ mixture present *in vivo*.
315

316 **Development of an anti-toxic-turn antibody, 24B3, and its application towards AD**
317 **diagnosis**

318 To identify the molecular species of Aβ oligomers that show neurotoxicity, it is
319 necessary to extract and purify applicable Aβ oligomers from human brain or
320 cerebrospinal fluid (CSF). However, structure–function analysis of Aβ oligomers is
321 problematic because Aβ oligomers are in complex equilibrium among monomers,

oligomers, and fibrils. To address this problem, anti-Aβ oligomer antibodies that recognize the specific tertiary structure of each oligomer would be useful. Several anti-Aβ oligomer antibodies have been developed, and some are widely used for Aβ research. For example, A11 polyclonal antibody reacts with toxic oligomers of Aβ42 more strongly than its fibrillar aggregates [81]. Attention has also been given to NU1 as an Aβ oligomer-specific antibody [82]. Moreover, anti-oligomeric (anti-protofibrillar) Aβ antibody (BAN2401) has been developed for the treatment of AD [83]. The weak point of these antibodies is that their epitopes are not clarified, and thus their usage in oligomer analyses has several limitations.

My colleagues and I focused on the toxic turn of Aβ42 at position 22 and 23, which could be mimicked by proline substitution. At first, we obtained 11A1 antibody by immunization to mice with E22P-Aβ10-35 bound to a carrier protein [84]. 11A1 antibody reacted not only with extracellular Aβ aggregates (senile plaques) but also with intracellular Aβ aggregates, some of which were considered to be toxic oligomers. Notably, intracellular Aβ oligomers were clearly detected in neurons differentiated from induced pluripotent stem cells of AD patients [85]. However, reactivity of 11A1 against senile plaques and monomeric Aβ was also high, making it difficult to use this antibody as a diagnostic tool for AD.

Next, we focused on 24B3 antibody [57], which was obtained along with 11A1 by screening using E22P-Aβ42. This reacted strongly with E22P-Aβ42 and the dimer models, **3** and **4**, but unlike 11A1, hardly bound to wild-type Aβ42 [57]. It was notable that preincubated wild-type Aβ42 was recognized by 24B3, indicating that toxic oligomers derived from wild-type Aβ42 could also bind to 24B3. These results prompted us to generate a sandwich enzyme-linked immunosorbent assay (ELISA) in collaboration

with Immuno-Biological Laboratories (IBL) Co., Ltd., for potential application in early AD diagnosis, since formation of toxic Aβ oligomers is considered to be an initial event of AD [23-25]. After several trials, 82E1 [86], which recognizes the N-terminal-end of Aβ, was fixed to a solid-phase for capture, while 24B3 conjugated with horseradish peroxidase for detection was used for quantification of toxic oligomers with a toxic Aβ turn in human CSF. To prove the concept of the "toxic-conformer theory", human CSF was analyzed using this ELISA in collaboration with Professor Takahiko Tokuda at Kyoto Prefectural University of Medicine [57]. As shown in Figure 11, the ratio of toxic conformer to total Aβ42 in AD/mild cognitive impairment (MCI) patients was significantly higher compared with age-matched non-AD controls. Nonetheless, a significant difference in the amount of toxic conformer between AD/MCI and control groups was not observed, possibly because of the small number of samples. Indeed, Akiba *et al.*, [87] reported significantly high levels of the toxic conformer in AD patients using our ELISA kit. They also suggested that the ratio of toxic conformer to total Aβ42 in patients with idiopathic normal pressure hydrocephalus (iNPH) was significantly higher than control groups. This indicates that the toxic conformer ratio could be a reliable biomarker for predicting the likelihood of patients with iNPH progressing into AD.

The 24B3 and 11A1 antibodies significantly suppressed neurotoxicity induced by Aβ42 and E22P-Aβ42, whereas 82E1 and 4G8 (sequence-specific antibodies against region 18–23 of Aβ) [88] did not [57]. The protective effect of 24B3 was higher than 11A1. Based on these results, passive immunization of 24B3 against AD model mice (Tg2576) was examined in collaboration with Dr. Takahiko Shimizu at Chiba University [89]. Intraperitoneal administration for 3 months (10 mg/kg/week) improved cognitive impairment, although the number of senile plaques did not change. Moreover, even single intravenous administration (20 mg/kg) suppressed the memory deficit. Masking of toxic

oligomers by 24B3 could lead to effective AD therapies with little adverse effects if 24B3 was reproduced for human use.

To investigate the contribution of the toxic conformer with the toxic turn to AD pathogenesis, in collaboration with Dr. Shimizu, we recently developed a new AD mouse model with E22P-Aβ mutation using a knock-in technique to avoid the artificial phenotype observed in transgenic-type model mice [90]. Interestingly, a trimer band and high molecular-weight oligomer bands (but not a monomer band) were detected in a Tris buffer-soluble fraction of E22P-Aβ knock-in mice at six months of age, when cognitive impairment occurred in the novel object recognition test. These data suggest that the toxic conformer of Aβ induced cognitive dysfunction mediated by toxic oligomer formation. However, loss of neurons was not observed in these model mice, indicating that Aβ oligomers induced only synapse toxicity such as inhibition of LTP without severe neurotoxic effects. Onset of AD might require accumulation of toxic Aβ oligomers, followed by hyper-phosphorylation of tau proteins. Toxic oligomers might act as mediators for tau phosphorylation to result in neuronal loss. In this context, E22P-Aβ knock-in mice would be a useful model for evaluating oligomer-induced cognitive impairment in AD. In addition, synapse toxicity of the trimer models (**5**–**7**) should also be evaluated.

Summary and future perspectives

As described, the antibody 24B3 developed on the basis of the "toxic conformation theory" could be a useful tool for early diagnosis of AD. The next step is to optimize this antibody based on X-ray crystallographic analysis of the hapten peptide and its Fab domain complex. Structural optimization of the toxic dimer and trimer models for second generation antibodies against toxic oligomers of Aβ is also a pressing need. Recently,

attention has been given to AD diagnosis using human plasma samples instead of CSF, which is more invasive. Yanagisawa and colleagues proposed new analytical methods to quantify the amount of Aβ peptides in plasma samples using mass spectrometry to predict accumulation of Aβ in the brain [91]. Our own approach is to use a Simoa™ (single molecule array) technology. Using this technology, Tokuda and colleagues established the method to quantify the amount of phosphorylated-tau (p-tau) in human plasma, and showed that p-tau levels were significantly higher in AD patients than non-AD controls [92]. In collaboration with Professor Tokuda and Professor Juan C. Troncoso at the Johns Hopkins University School of Medicine, we are measuring the amount of toxic conformer in human plasma samples using Simoa™ technology (unpublished results).

Prevention and treatment of AD are indispensable after diagnosis of early onset. It has been reported that many natural products (mainly flavonoids) suppress aggregation and neurotoxicity of Aβ42 [93,94]. However, their mechanism of action remains unknown. Recently, we proposed three structural features required for suppression of Aβ42 aggregation [95]. These features are: a catechol moiety that reacts with Lys residues of Aβ42 after oxidation [96], planarity due to α,β-unsaturated carbonyl groups that ensure intercalation of the molecule into the intermolecular β-sheet region in Aβ aggregates [97,98], and carboxy groups of triterpenoids or anthraqinoids that form salt bridges with Lys16 of Aβ42 oligomers [99,100]. These structural features would be useful for predicting new anti-Aβ42 aggregative compounds from natural sources, which might become promising lead compounds for protection against early onset of AD.

Treatment of AD is also a pressing need. Immunotherapy using anti-Aβ antibodies has been extensively investigated [101,102] after pioneering work by Schenk and colleagues in 1999 [103]. However, most attempts gave disappointing results. Possible reasons for this might be that the antibodies used were not optimized for toxic species of

421 Aβ aggregates, and that administration time of the antibodies to AD patients was too late.
422 Although application of our 24B3 antibody [57] might be promising, considerable money
423 is required for drug development and antibody therapy. In addition, γ-secretase and β-
424 secretase inhibitors have also failed in clinical trials [104].

425 Another therapeutic approach has been performed using PKC activators. Cumulative
426 evidence suggests that inhibition of PKCα decreases the amount of Aβ42 and Aβ40, and
427 that activation of PKCε enhances degradation of Aβ through endothelin converting
428 enzyme [105-107]. Bryostatin 1, isolated from bryozoan [108], is one of the most
429 promising PKC activators because of its low adverse effects such as tumor promotion and
430 proinflammatory activity [107,109]. However, low availability from natural sources and
431 structural complexity has hampered the supply for medicinal leads. To overcome these
432 issues, synthesis of simplified analogs of bryostatin 1 that potently activate PKC
433 [110,111], and practical synthetic methods of bryostatin 1 have been reported [112,113].
434 Our own approach was to develop new medicinal leads from naturally occurring PKC
435 ligands, phorbol esters, ingenol esters, teleocidins, and aplysiatoxins [114]. After
436 extensive structure–activity studies, aplysiatoxins were found to be the most promising
437 leads [115] since their hydrophobicity is relatively low, and their structure is regarded as
438 a conformationally-fixed analogue of diacylglycerol, an endogenous ligand for PKC
439 isozymes. Moreover, we have developed 10-Me-Aplog-1 [116], a simplified analogue of
440 aplysiatoxin isolated from sea hare [117], as a new PKC activator without tumor-
441 promoting and proinflammatory activities (Figure 12). Since 10-Me-Aplog-1 did not
442 show any tumor-promoting and proinflammatory activities, it might be effective for
443 decreasing toxic oligomers of Aβ.

444 I felt something like my destiny when I began to synthesize a simplified analogue of
445 aplysiatoxin as a surrogate of bryostatin 1 with Dr. Yu Nakagawa in 2007. My research

on the chemistry and biology of Aβ originated from the structural study of PKC C1 domains through peptide synthesis. Additionally, research on the treatment of AD connected again with research on naturally occurring PKC ligands. That is why research is interesting generally.

Acknowledgements

I would like to express many thanks to the staff and graduate students who worked with me in the laboratory of Organic Chemistry in Life Sciences, Division of Food Science & Biotechnology, Graduate School of Agriculture, Kyoto University, and to all the collaborators in this study, most of them mentioned in the text and shown in the references.

I would like to express my sincere thanks to Dr. Koichi Koshimizu, emeritus professor of Kyoto University, for giving me the opportunity to study teleocidins, which was the starting point for this study. At the beginning of this study, Dr. Hideo Hayashi, emeritus professor of Osaka Prefectural University, provided much help and encouragement. I would also like to thank Dr. Hajime Ohigashi, emeritus professor of Kyoto University, for continuous support of my research. Finally, I would like to thank the Japan Society for Bioscience, Biotechnology, and Agrochemistry (JSBBA) for awarding me the JSBBA Award 2019.

I thank Rachel James, Ph.D., from Edanz Group (www.edanzediting.com/ac) for editing a draft of this manuscript.

Disclosure statement

No potential conflict of interest was reported by the author.

Funding

This work was supported in part by Grants-in-Aid for Scientific Research (S) (26221202), (A) (19H00921, 21258015, 18208011), (B) (16380080, 13460048), (C) (11660109), Scientific Research on Innovative Areas “Frontier Research on Chemical Communications (17H06405), and “Chemical Biology of Natural Products” (23102011) from JSPS. This work was also supported in part by funds from The Uehara Memorial Foundation, The Naito Science & Engineering Foundation, The Takeda Science Foundation, and Asahi Group Foundation.

References

[1] Irie K, Hirota M, Hagiwara N, et al. The Epstein-Barr virus early antigen-inducing indole alkaloids, (–)-indolactam V and its related compounds, produced by Actinomycetes. Agric Biol Chem. 1984;48:1269-1274.

[2] Endo Y, Shudo K, Okamoto T. Molecular requirements for epigenetic modulators. Synthesis of active fragments of teleocidins and lyngbyatoxin. Chem Pharm Bull. 1982;30:3457-3460.

[3] Takashima M, Sakai H. A new toxic substance, teleocidin, produced by *Streptomyces*. Part I. Production, isolation and chemical studies. Bull Agr Chem Soc Jpn. 1960;24:647-651.

[4] Nakata H, Harada H, Hirata Y. The structure of teleocidin B. Tetrahedron Lett. 1966;23:2515-2522.

[5] Hitotsuyanagi Y, Fujiki H, Suganuma M, et al. Isolation and structure elucidation of teleocidin B-1, B-2, B-3 and B-4. Chem Pharm Bull. 1984;32:4233-4236.

[6] Fujiki H, Sugimura T. New class of tumor promoters: teleocidin, aplysiatoxin, and palytoxin. Adv Cancer Res. 1987;49:223-264.

[7] Heikkilä J, Akerman KE. (–)-Indolactam V activates protein kinase C and induces changes in muscarinic receptor functions in SH-SY5Y human neuroblastoma cells. Biochem Biophys Res Commun. 1989;162:1207-1213.

[8] Nishizuka Y. Protein kinase C and lipid signaling for sustained cellular responses. FASEB J. 1995;9:484-496.

[9] Irie K, Koshimizu K. Chemistry of indole alkaloid tumor promoter teleocidins. Comments Agric Food Chem. 1993;3:1-25.

519 [10] Irie K. Chemical studies on tumor promoter teleocidins: structure-activity
520 relationship and photoaffinity labeling. Nippon Nogeikagaku Kaishi. 1994;68:1289-
521 1296.
522 [11] Ono Y, Fujii T, Igarashi K, et al. Phorbol ester binding to protein kinase C requires
523 a cysteine-rich zinc-finger-like sequence. Proc Natl Acad Sci USA. 1989;86:4868-
524 4871.
525 [12] Hurley JH, Newton AC, Parker PJ, et al. Taxonomy and functions of C1 protein
526 kinase C homology domains. Protein Sci. 1997;6:477-480.
527 [13] Zhang G, Kazanietz MG, Blumberg PM, et al. Crystal structure of the Cys2 activator-
528 binding domain of protein kinase Cδ in complex with phorbol ester. Cell.
529 1995;81:917-924.
530 [14] Wender PA, Irie K, Miller BL. Identification, activity, and structural studies of
531 peptides incorporating the phorbol ester-binding domain of protein kinase C. Proc
532 Natl Acad Sci USA. 1995;92:239-243.
533 [15] Irie K, Oie K, Nakahara A, et al. Molecular basis for protein kinase C isozyme-
534 selective binding: the synthesis of the cysteine-rich domains of all protein kinase C
535 isozymes. J Am Chem Soc. 1998;120:9159-9167.
536 [16] Irie K, Nakahara A, Nakagawa Y, et al. Establishment of a binding assay for protein
537 kinase C isozymes using synthetic C1 peptides and development of new medicinal
538 leads with protein kinase C isozyme and C1 domain selectivity. Pharm Ther.
539 2002;93:271-281.
540 [17] Irie K, Nakagawa Y, Ohigashi H. Toward the development of new medicinal leads
541 with selectivity for protein kinase C isozymes. Chem Rec. 2005;5:185-195.
542 [18] Shindo M, Irie K, Masuda A, et al. Synthesis and phorbol ester binding of the
543 cysteine-rich domains of diacylglycerol kinase (DGK) isozymes. DGKγ and DGKβ

544 are new targets of tumor-promoting phorbol esters. J Biol Chem. 2003;278:18448-
545 18454.
546 [19] Fukuda H, Irie K, Nakahara A, et al. Solid-phase synthesis, mass spectrometric
547 analysis of the zinc-folding, and phorbol ester-binding studies of the 116-mer peptide
548 containing the tandem cysteine-rich C1 domains of protein kinase C gamma. Bioorg
549 Med Chem. 1999;7:1213-1221.
550 [20] Carpino LA. 1-Hydroxy-7-azabenzotriazole. An efficient peptide coupling additive.
551 J Am Chem Soc. 1993;115:4397-4398.
552 [21] Haass C, Selkoe DJ. Soluble protein oligomers in neurodegeneration: lessons from
553 the Alzheimer's amyloid beta-peptide. Nat Rev Mol Cell Biol. 2007;8:101-112.
554 [22] Selkoe DJ, Hardy J. The amyloid hypothesis of Alzheimer's disease at 25 years.
555 EMBO Mol Med. 2016;8:595-608.
556 [23] Walsh DM, Klyubin I, Fadeeva JV, et al. Naturally secreted oligomers of amyloid β
557 protein potently inhibit hippocampal long-term potentiation in vivo. Nature.
558 2002;416:535-539.
559 [24] Benilova I, Karran E, De Strooper B. The toxic Aβ oligomer and Alzheimer's
560 disease: an emperor in need of clothes. Nat Neurosci. 2012;15:349-357.
561 [25] Ono, K. Alzheimer's disease as oligomeropathy. Neurochem Int. 2018;119:57-70.
562 [26] Petkova AT, Ishii Y, Balbach JJ, et al. A structural model for Alzheimer's β-amyloid
563 fibrils based on experimental constraints from solid state NMR. Proc Natl Acad Sci
564 USA. 2002;99:16742-16747.
565 [27] Xiao Y, Ma B, McElheny D, et al. Aβ(1-42) fibril structure illuminates self-
566 recognition and replication of amyloid in Alzheimer's disease. Nat Struct Mol Biol.
567 2015;22:499-505.

[28] Colvin MT, Silvers R, Ni QZ, et al. Atomic resolution structure of monomorphic Aβ42 amyloid fibrils. J Am Chem Soc. 2016;138:9663-9674.

[29] Wälti MA, Ravotti F., Arai H, et al. Atomic-resolution structure of a disease-relevant Aβ(1-42) amyloid fibril. Proc Natl Acad Sci USA. 2016;113:E4976-E4984.

[30] Wood SJ, Wetzel R, Martin JD, et al. Prolines and amyloidogenicity in fragments of the Alzheimer's peptide β/A4. Biochemistry. 1995;34:724-730.

[31] Morimoto A, Irie K, Murakami K, et al. Aggregation and neurotoxicity of mutant amyloid β (Aβ) peptides with proline replacement: importance of turn formation at positions 22 and 23. Biochem Biophys Res Commun. 2002;295:306-311.

[32] Morimoto A, Irie K, Murakami K, et al. Analysis of the secondary structure of β-amyloid (Aβ42) fibrils by systematic proline replacement. J Biol Chem. 2004;279:52781-52788.

[33] Murakami K, Irie K, Morimoto A, et al. Neurotoxicity and physicochemical properties of Aβ mutant peptides from cerebral amyloid angiopathy: implication for the pathogenesis of cerebral amyloid angiopathy and Alzheimer's disease. J Biol Chem. 2003;278:46179-46187.

[34] Izuo N, Kume T, Sato M, et al. Toxicity in rat primary neurons through the cellular oxidative stress induced by the turn formation at positions 22 and 23 of Aβ42. ACS Chem Neurosci. 2012;3:674-681.

[35] Masuda Y, Uemura S, Nakanishi A, et al. Verification of the C-terminal intramolecular β-sheet in Aβ42 aggregates using solid-state NMR: implications for potent neurotoxicity through the formation of radicals. Bioorg Med Chem Lett. 2008;18:3206-3210.

591 [36] Irie K, Murakami K, Masuda Y, et al. Structure of β-amyloid fibrils and its relevance
592 to their neurotoxicity: implications for the pathogenesis of Alzheimer's disease. J
593 Biosci Bioeng. 2005;99:437-447.
594 [37] Barnham KJ, Haeffner F, Ciccotosto GD, et al. Tyrosine gated electron transfer is
595 key to the toxic mechanism of Alzheimer's disease of β-amyloid. FASEB J.
596 2004;18:1427-1429.
597 [38] Varadarajan S, Yatin S, Kanski J, et al. Methione residue 35 is important in amyloid
598 β-peptide-associated free radical oxidative stress. Brain Res Bull. 1999;50:133-141.
599 [39] Varadarajan S, Kanski J, Aksenova M, et al. Different mechanisms of oxidative
600 stress and neurotoxicity for Alzheimer's Aβ(1-42) and Aβ(25-35). J Am Chem Soc.
601 2001;123:5625-5631.
602 [40] Curtain CC, Ali F, Volitakis I, et al. Alzheimer's disease amyloid-β binds copper
603 and zinc to generate an allosterically ordered membrane-penetrating structure
604 containing superoxide dismutase-like subunits. J Biol Chem. 2001;276:20466-20473.
605 [41] Murakami K, Hara H, Masuda Y, et al. Distance measurement between Tyr10 and
606 Met35 in amyloid β by site-directed spin-labeling ESR spectroscopy: implications for
607 the stronger neurotoxicity of Aβ42 than Aβ40. ChemBioChem. 2007;8:2308-2314.
608 [42] Murakami K, Irie K, Ohigashi H, et al. Formation and stabilization model of the 42-
609 mer Aβ radical: implications for the long-lasting oxidative stress in Alzheimer's
610 disease. J Am Chem Soc. 2005;127:15168-15174.
611 [43] Takegoshi K, Nakamura S, Terao T. ^{13}C-^{1}H dipolar-assisted rotational resonance in
612 magic-angle spinning NMR. Chem Phys Lett. 2001;344:631-637.
613 [44] Takegoshi K, Nakamura S, Terao T. ^{13}C-^{1}H dipolar driven ^{13}C-^{13}C recoupling
614 without ^{13}C rf irradiation in nuclear magnetic resonance of rotating solids. J Chem
615 Phys. 2003;118:2325-2341.

[45] Miravalle L, Tokuda T, Chiarle R, et al. Substitutions at codon 22 of Alzheimer's A peptide induce diverse conformational changes and apoptotic effects in human cerebral endothelial cells. J Biol Chem. 2000;275: 27110-27116.

[46] Masuda Y, Irie K, Murakami K, et al. Verification of the turn at positions 22 and 23 of the beta-amyloid fibrils with Italian mutation using solid-state NMR. Bioorg Med Chem. 2005;13:6803-6809.

[47] Masuda Y, Uemura S, Ohashi R, et al. Identification of physiological and toxic conformations in Aβ42 aggregates. ChemBioChem. 2009;10:287-295.

[48] De Strooper B. Proteases and proteolysis in Alzheimer's disease: a multifactorial view on the disease process. Physiol Rev. 2010;90:465-494.

[49] Williams AD, Portelius E, Kheterpal I, et al. Mapping Aβ amyloid fibril secondary structure using scanning proline mutagenesis. J Mol Biol. 2004;335:833-842.

[50] Ono K, Condron MM, Teplow DB. Structure-neurotoxicity relationships of amyloid β-protein oligomers. Proc Natl Acad Sci USA 2009;106:14745-14750.

[51] Kok WM, Scanlon DB, Karas JA, et al. Solid-phase synthesis of homodimeric peptides: preparation of covalently-linked dimers of amyloid β peptides. Chem Commun. 2009;6228-6230.

[52] O'Nuallain B, Freir DB, Nicoll AJ, et al. Amyloid β-protein dimers rapidly form stable synaptotoxic protofibrils. J Neurosci. 2010;30:14411-14419.

[53] Yamaguchi T, Yagi H, Goto Y, et al. A disulfide-linked amyloid-β peptide dimer forms a protofibril-like oligomer through a distinct pathway from amyloid fibril formation. Biochemistry. 2010;49:7100-7107.

[54] Kok WM, Cottam JM, Ciccotosto GD, et al. Synthetic dityrosine-linked β-amyloid dimers form stable, soluble, neurotoxic oligomers. Chem Sci. 2013;4:4449-4454.

[55] O'Malley TT, Oktaviani NA, Zhang D, et al. Aβ dimers differ from monomers in structural propensity, aggregation paths and population of synaptotoxic assemblies. Biochem J. 2014;461:413-426.

[56] Irie Y, Murakami K, Hanaki M, et al. Synthetic models of quasi-stable amyloid β40 oligomers with significant neurotoxicity. ACS Chem Neurosci. 2017;8:807-816.

[57] Murakami K, Tokuda M, Suzuki T, et al. Monoclonal antibody with conformational specificity for a toxic conformer of amyloid β42 and its application toward the Alzheimer's disease diagnosis. Sci Rep. 2016;6:29038.

[58] Masuda Y, Nakanishi A, Ohashi R, et al. Verification of the intermolecular parallel β-sheet in E22K-Aβ42 aggregates by solid-state NMR using rotational resonance: implications for the supramolecular arrangement of the toxic conformer of Aβ42. Biosci Biotechnol Biochem. 2008;72:2170-2175.

[59] Paradisi F, Porzi G, Rinaldi S, et al. A simple asymmetric synthesis of (+)- and (–)-2,6-diaminopimelic acids. Tetrahedron: Asymmetry. 2000;11:1259-1262.

[60] Watt AD, Perez KA, Rembach A, et al. Oligomers, fact or artefact? SDS-PAGE induces dimerization of β-amyloid in human brain samples. Acta Neuropathol. 2013;125:549-564.

[61] Bernstein SL, Dupuis NF, Lazo ND, et al. Amyloid-β protein oligomerization and the importance of tetramers and dodecamers in the aetiology of Alzheimer's disease. Nat Chem. 2009;1:326-331.

[62] Kloniecki M, Jablonowska A, Poznanski J, et al. Ion mobility separation coupled with MS detects two structural states of Alzheimer's disease Aβ1-40 peptide oligomers. J Mol Biol. 2011;407:110-124.

[63] Österlund N, Moons R, Ilag LL, et al. Native ion mobility-mass spectrometry reveals the formation of β-barrel shaped amyloid-β hexamers in a membrane-mimicking environment. J Am Chem Soc. 2019;141:10440-10450.

[64] Klyubin I, Betts V, Wetzel AT, et al. Amyloid β protein dimer-containing human CSF disrupts synaptic plasticity: prevention by systemic passive immunization. J Neurosci. 2008;28:4231-4237.

[65] Shankar GM, Li S, Mehta TH, et al. Amyloid-β protein dimers isolated directly from Alzheimer's brains impair synaptic plasticity and memory. Nat Med. 2008;14:837-842.

[66] Lendel C, Bjerring M, Dubnovitsky A, et al. A hexameric peptide barrel as building block of amyloid-β protofibrils. Angew Chem Int Ed. 2014;53:12756-12760.

[67] Townsend M, Shankar GM, Mehta T, et al. Effects of secreted oligomers of amyloid β-protein on hippocampal synaptic plasticity: a potent role for trimers. J Physiol. 2006;572:477-492.

[68] Tomiyama T, Nagata T, Shimada H, et al. A new amyloid β variant favoring oligomerization in Alzheimer's-type dementia. Ann. Neurol. 2008;63:377-387.

[69] Spencer RK, Li H, Nowick JS. X-ray crystallographic structures of trimers and higher-order oligomeric assemblies of a peptide derived from Aβ(17-36). J Am Chem Soc. 2014;136:5595-5598.

[70] Shinoda K, Sohma Y, Kanai M. Synthesis of chemically-tethered amyloid-β segment trimer possessing amyloidogenic properties. Bioorg Med Chem Lett. 2015;25:2976-2979.

[71] Huang D, Zimmerman MI, Martin PK, et al. Antiparallel β-sheet structure within the C-terminal region of 42-residue Alzheimer's amyloid-β peptides when they form 150-kDa oligomers. J Mol Biol 2015;427:2319-2328.

688 [72] Irie Y, Hanaki M, Murakami K, et al. Synthesis and biochemical characterization of
689 quasi-stable trimer models of full-length amyloid β40 with a toxic conformation.
690 Chem Commun. 2019;55:182-185.
691 [73] Ritzén A, Basu B, Wållberg A, et al. Phenyltrisalanine: a new, C_3-symmetric,
692 trifunctional amino acid. Tetrahedron: Asymmetry. 1998:3491-3496.
693 [74] Imamoto T, Tamura K, Zhang Y, et al. Rigid P-chiral phosphine ligands with *tert*-
694 butylmethylphosphino groups for rhodium-catalyzed asymmetric hydrogenation of
695 functionalized alkenes. J Am Chem Soc. 2012;134:1754-1769.
696 [75] Wogulis M, Wright S, Cunningham D, et al. Nucleation-dependent polymerization
697 is an essential component of amyloid-mediated neuronal cell death. J Neurosci.
698 2005;25:1071-1080.
699 [76] Lambert MP, Barlow AK, Chromy BA, et al. Diffusible, nonfibrillar ligands derived
700 from $A\beta_{1-42}$ are potent central nervous system neurotoxins. Proc Natl Acad Sci USA.
701 1998;95:6448-6453.
702 [77] Deshpande A, Mina E, Glabe C, et al. Different conformations of amyloid β induce
703 neurotoxicity by distinct mechanisms in human cortical neurons. J Neurosci.
704 2006;26:6011-6018.
705 [78] Lesné S, Koh MT, Kotilinek L, et al. A specific amyloid-β protein assembly in the
706 brain impairs memory. Nature. 2006;440:352-357.
707 [79] Harper JD, Wong SS, Lieber CM, et al. Observation of metastable Aβ amyloid
708 protofibrils by atomic force microscopy. Chem Biol. 1997;4:119-125.
709 [80] Noguchi A, Matsumura S, Dezawa M, et al. Isolation and characterization of patient-
710 derived, toxic, high mass amyloid β-protein (Aβ) assembly from Alzheimer's disease
711 brains. J Biol Chem. 2009;284:32895-32905.

712 [81] Kayed R, Head E, Thompson JL, et al. Common structure of soluble amyloid
713 oligomers implies common mechanism of pathogenesis. Science 2003;300:486-489.
714 [82] Lambert MP, Velasco PT, Chang L, et al. Monoclonal antibodies that target
715 pathological assemblies of Aβ. J Neurochem. 2007;100:23-35.
716 [83] Logovinsky V, Satlin A, Lai R, et al. Safety and tolerability of BAN2401 – a clinical
717 study in Alzheimer's disease with a protofibril selective Aβ antibody. Alzheimers Res
718 Ther. 2018;8:14.
719 [84] Murakami K, Horikoshi-Sakuraba Y, Murata N, et al. Monoclonal antibody against
720 the turn of the 42-residue amyloid β-protein at positions 22 and 23. ACS Chem
721 Neurosci. 2010;1:747-756.
722 [85] Kondo T, Asai M, Tsukita K, et al. Modeling Alzheimer's disease with iPSCs reveals
723 stress phenotypes associated with intracellular Aβ and differential drug
724 responsiveness. Cell Stem Cell. 2013;12:487-496.
725 [86] Horikoshi Y, Mori T, Maeda M, et al. Aβ N-terminal-end specific antibody reduced
726 β-amyloid in Alzheimer-model mice. Biochem Biophys Res Commun.
727 2004;325:384-387.
728 [87] Akiba C, Nakajima M, Miyajima M, et al. Change of amyloid-β 1-42 toxic
729 conformer ratio after cerebrospinal fluid diversion predicts long-term cognitive
730 outcome in patients with idiopathic normal pressure hydrocephalus. J Alzheimers Dis.
731 2018;63:989-1002.
732 [88] Hatami A, Monjazeb S, Glabe C. The anti-amyloid-β monoclonal antibody 4G8
733 recognizes a generic sequence-independent epitope associated with α-synuclein and
734 islet amyloid polypeptide amyloid fibrils. J Alzheimers Dis. 2016;50:517-525.
735 [89] Izuo N, Kasahara C, Murakami K, et al. A toxic conformer of Aβ42 with a turn at
736 22-23 is a novel therapeutic target for Alzheimer's disease. Sci Rep. 2017;7:11811.

[90] Izuo N, Murakami K, Fujihara Y, et al. An *App* knock-in mouse inducing the formation of a toxic conformer of Aβ as a model for evaluating only oligomer-induced cognitive decline in Alzheimer's disease. Biochem Biophys Res Commun. 2019;515:462-467.

[91] Nakamura A, Kaneko N, Villemagne V, et al. High performance plasma amyloid-β biomarkers for Alzheimer's disease. Nature. 2018;554:249-254.

[92] Tatebe H, Kasai T, Ohmichi T, et al. Quantification of plasma phosphorylated tau to use as a biomarker for brain Alzheimer pathology: pilot case-control studies including patients with Alzheimer's disease and down syndrome. Mol Neurodegener. 2017;12:63.

[93] Williams RJ, Spencer JP. Flavonoids, cognition, and dementia: actions, mechanisms, and potential therapeutic utility for Alzheimer disease. Free Radic Biol Med. 2012;52:35-45.

[94] Williams P, Sorribas A, Howes MJ. Natural products as a source of Alzheimer's drug leads. Nat Prod Rep. 2011;28:48-77.

[95] Murakami K, Irie K. Three structural features of functional food components and herbal medicine with amyloid β42 anti-aggregation properties. Molecules 2019;24:E2125.

[96] Sato M, Murakami K, Uno M, et al. Site-specific inhibitory mechanism for amyloid β42 aggregation by catechol-type flavonoids targeting the Lys residues. J Biol Chem. 2013;288:23212-23224.

[97] Hanaki M, Murakami K, Akagi K, et al. Structural insights into mechanisms for inhibiting amyloid β42 aggregation by non-catechol-type flavonoids. Bioorg Med Chem. 2016;24:304-313.

761 [98] Hanaki M, Murakami K, Katayama S, et al. Mechanistic analyses of the suppression
762 of amyloid β42 aggregation by apomorphine. Bioorg Med Chem. 2018;26:1538-
763 1546.
764 [99] Yoshioka T, Murakami K, Ido K, et al. Semisynthesis and structure-activity studies
765 of uncarinic acid C isolated from *Uncaria rhynchophylla* as a specific inhibitor of the
766 nucleation phase in amyloid β42 aggregation. J Nat Prod. 2016;79:2521-2529.
767 [100] Murakami K, Yoshioka T, Horii S, et al. Role of the carboxy groups of triterpenoids
768 in their inhibition of the nucleation of amyloid β42 required for forming toxic
769 oligomers. Chem Commun. 2018;54:6272-6275.
770 [101] van Dyck CH. Anti-amyloid-β monoclonal antibodies for Alzheimer's disease:
771 pitfalls and promise. Biol Psychiatry. 2018;83:311-319.
772 [102] Panza F, Lozupone M, Logroscino G, et al. A critical appraisal of amyloid-β-
773 targeting therapies for Alzheimer disease. Nat Rev Neurol. 2019;15:73-88.
774 [103] Schenk D, Barbour R, Dunn W, et al. Immunization with amyloid-β attenuates
775 Alzheimer-disease-like pathology in the PDAPP mouse. Nature. 1999;400:173-177.
776 [104] Panza F, Lozupone M, Dibello V, et al. Are antibodies directed against amyloid-β
777 (Aβ) oligomers the last call for the Aβ hypothesis of Alzheimer's disease?
778 Immunother. 2019;11:3-6.
779 [105] Choi DS, Wang D, Yu GQ, et al. PKCε increases endothelin converting enzyme
780 activity and reduces amyloid plaque pathology in transgenic mice. Proc Natl Acad
781 Sci USA. 2006;103:8215-8220.
782 [106] Khan TK, Nelson TJ, Verma VA, et al. A cellular model of Alzheimer's disease
783 therapeutic efficacy: PKC activation reverses Aβ-induced biomarker abnormality on
784 cultured fibroblasts. Neurobiol Dis. 2009;34:332-339.

785 [107] Nelson TJ, Alkon DL. Neuroprotective versus tumorigenic protein kinase C
786 activators. Trends Biochem Sci. 2009;34:136-145.
787 [108] Pettit GR, Herald CL, Doubek DL, et al. Isolation and structure of bryostatin 1. J
788 Am Chem Soc. 1982;104:6846-6848.
789 [109] Halford B. The bryostatins' tale. C&EN. 2011;89(43):10-17.
790 [110] Wender PA, Baryza JL, Bennett CE, et al. The practical synthesis of a novel and
791 highly potent analogue of bryostatin. J Am Chem Soc. 2002;124:13648-13649.
792 [111] Keck GE, Kraft MB, Truong AP, et al. Convergent assembly of highly potent
793 analogues of bryostatin 1 via pyran annulation: bryostatin look-alikes that mimic
794 phorbol ester function. J Am Chem Soc. 2008;130:6660-6661.
795 [112] Trost BM, Dong G. Total synthesis of bryostatin 16 using atom-economical and
796 chemoselective approaches. Nature. 2008;456:485-488.
797 [113] Wender PA, Hardman CT, Ho S, et al. Scalable synthesis of bryostatin 1 and
798 analogs, adjuvant leads against latent HIV. Science. 2017;358:218-223.
799 [114] Irie K, Yanagita RC. Synthesis and biological activities of simplified analogs of the
800 natural PKC ligands, bryostatin-1 and aplysiatoxin. Chem Rec. 2014;14:251-267.
801 [115] Nakagawa Y, Yanagita RC, Hamada N, et al. A simple analogue of tumor-
802 promoting aplysiatoxin is an antineoplastic agent rather than a tumor promoter:
803 development of a synthetically accessible protein kinase C activator with bryostatin-
804 like activity. J Am Chem Soc. 2009;131:7573-7579.
805 [116] Kikumori M, Yanagita RC, Tokuda H, et al. Structure-activity studies on the
806 spiroketal moiety of a simplified analogue of debromoaplysiatoxin with
807 antiproliferative activity. J Med Chem. 2012;55:5614-5626.

[117] Kato Y, Scheuer PJ. Aplysiatoxin and debromoaplysiatoxin, constituents of the marine mollusc *Stylocheilus longicauda* (Quoy and Gaimard, 1824). J Am Chem Soc 1974;96:2245-2246.

Figure captions

Figure 1. PKCδ-C1B domain peptide[15] and its crystal structure.[13]

Figure 2. Senile plaques and neurofibrillary tangles in brain slices of AD patients, along with Aβ42 and Aβ40 sequences.

Figure 3. The amyloid hypothesis.[22] MCI: mild cognitive impairment; AD: Alzheimer's disease.

Figure 4. Putative structure of dimers and trimers of Aβ42 induced by radicalization.[36,42] Green arrows show intra- or intermolecular β-sheet regions in Aβ42 aggregates.

Figure 5. Toxic or less toxic conformers of Aβ42.[47]

Figure 6. Structure of each monomer unit of aggregates of Aβ42[27-29] and Aβ40[26] revealed by solid-state NMR.

Figure 7. Putative structures of Aβ oligomers. It is not clear which oligomers are on-pathway, leading to amyloid fibrils, stable and less toxic species, and which oligomers are off-pathway, not resulting in fibril formation.

Figure 8. Structure of Aβ40 dimer models with a linker at position 30 or 38 and Aβ42 dimer with a linker at position 40. The Aβ40 dimer structure is based on proline scanning by Williams *et al.*[49] Green arrows show intermolecular β-sheet regions in Aβ40 aggregates.

Figure 9. Oligomer analysis of dimer and trimer models (**2**, **3**, **7**) by IM-MS after 4 h incubation at 12.5 μM for **2** and **3**, and 8 μM for **7** at 37 °C. *n* = number of dimers or trimers.

Figure 10. (A) Synthesis of (*S*,*S*,*S*)-tri-Fmoc-PtA. (a) 1,1,3,3-Tetramethyl guanidine, THF, 0 °C to room temperature, 4 h, 76%. (b) Rh-(*S*,*S*)-QuinoxP,[74] H_2 (4 atm), EtOAc/MeOH, room temperature, 4 h, 92% (>98%ee, >98%de). (c)

NaOHaq, MeOH, 1 h, 97%. (d) H_2, Pd/C, MeOH, overnight, 75%. (e) Fmoc-OSu, Na_2CO_3, MeCN, H_2O, 3 d, 50%.

(B) Structure of trimer models (**5**–**7**) of E22P-Aβ40.

Figure 11. Sandwich ELISA of cerebrospinal fluid from AD patients.[57]

Figure 12. Structure of aplysiatoxin and its simplified analogue, 10-Me-Aplog-1.[116]

HRFKVYNYMSPTFCDHCGSLLWGLVKQGLKCEDCGMNVHHKCREKVANLCG

1) Solid-phase synthesis
2) Zinc-folding

PKCδ-C1B

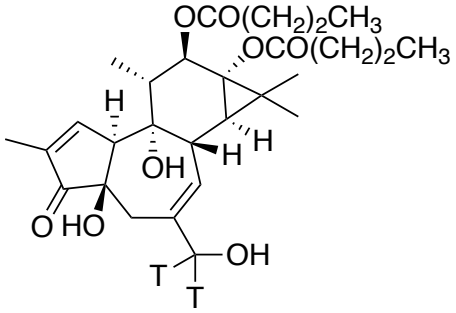

3) [^{3}H]PDBu binding assay

K_d = 0.53 nM

PKC ligand binding site

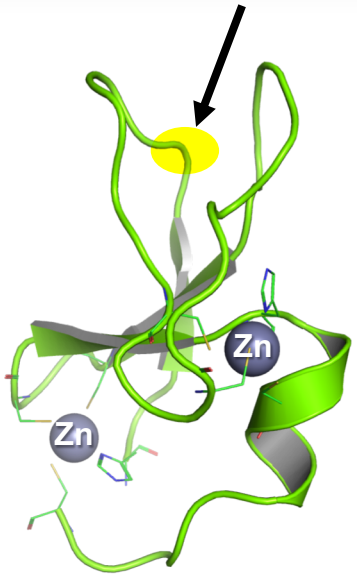

Crystal structure of δ-C1B

Figure 1

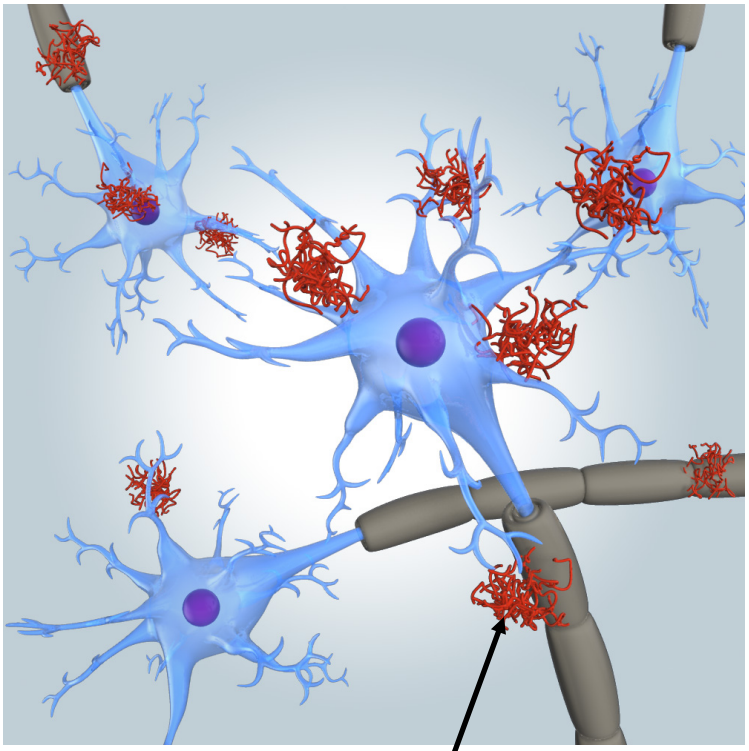

Senile plaques
(Aβ aggregates)

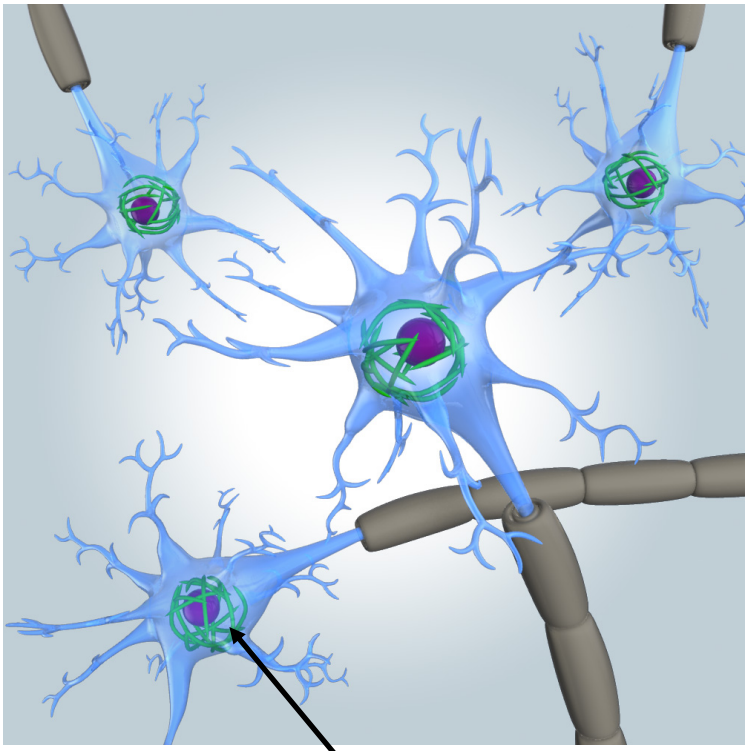

Neurofibrillary tangles

Aβ42: DAEFRHDSGY EVHHQKLVFF AEDVGSNKGA IIGLMVGGVV IA
Aβ40: DAEFRHDSGY EVHHQKLVFF AEDVGSNKGA IIGLMVGGVV

Figure 2

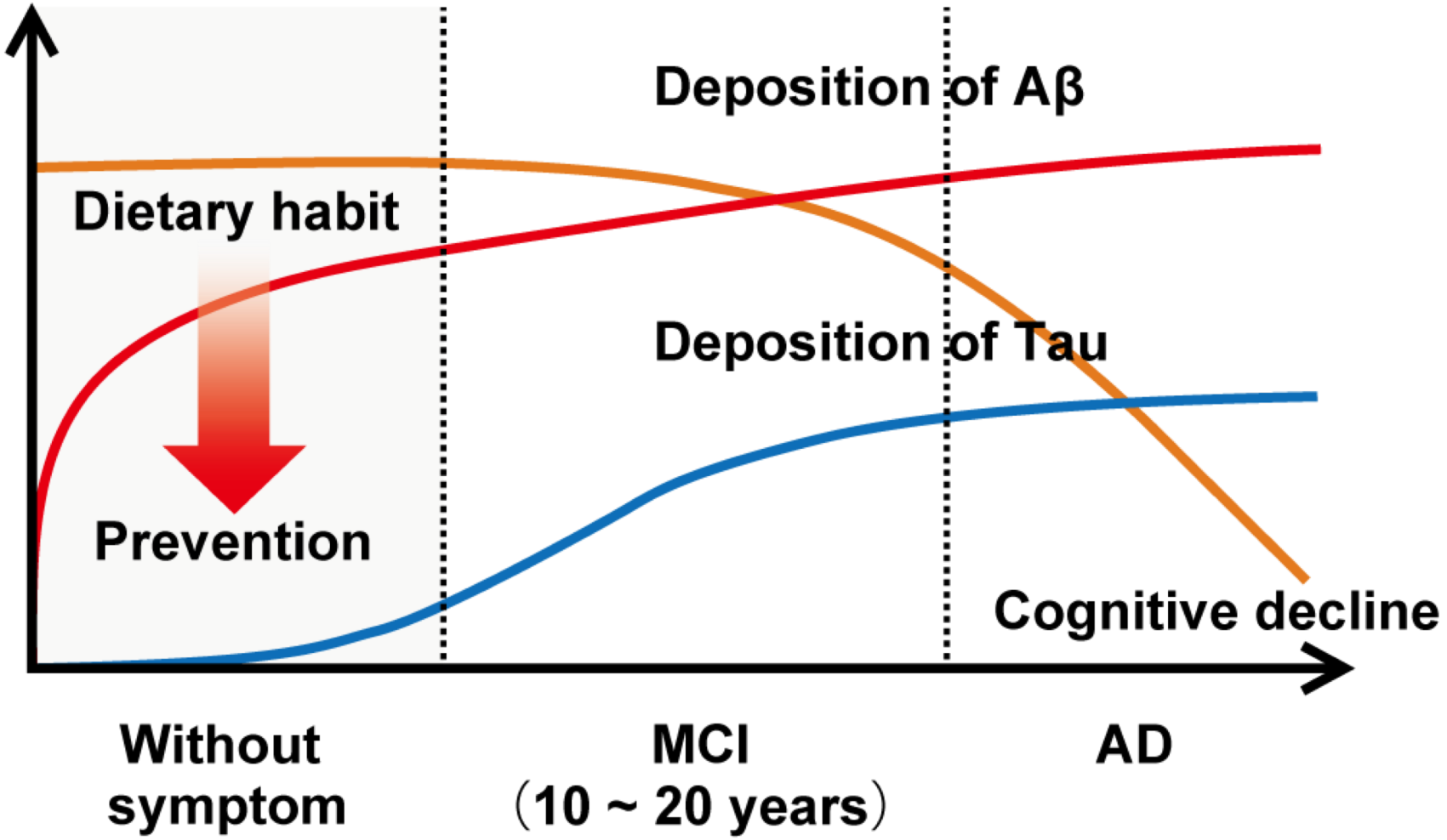
Deposition of Aβ
Dietary habit
Deposition of Tau
Prevention
Cognitive decline
Without symptom
MCI (10 ~ 20 years)
AD

Figure 3

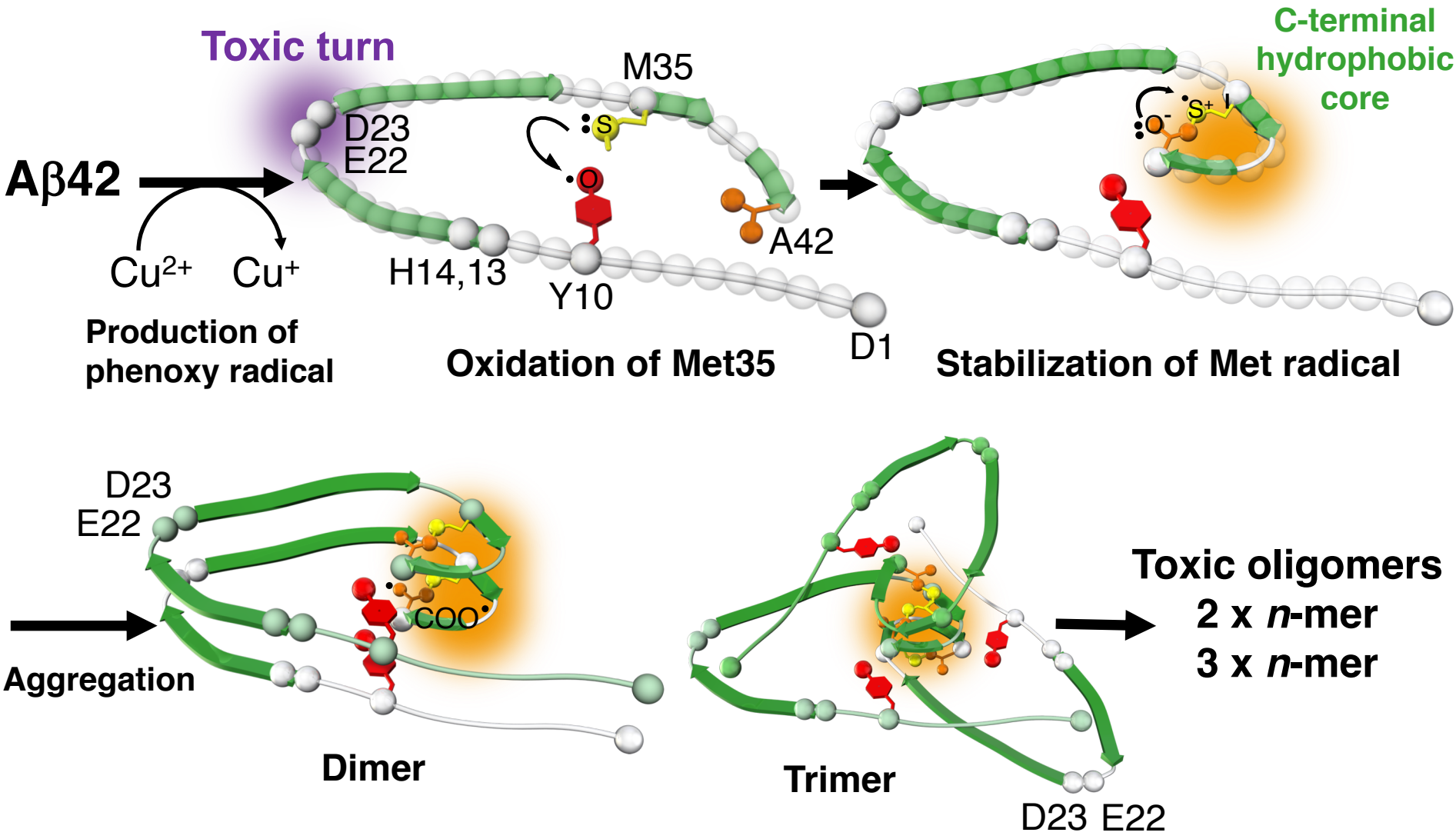
Toxic turn
M35
D23
E22
Aβ42
Cu2+
Cu+
H14,13
Y10
A42
D1
C-terminal
hydrophobic
core
Production of
phenoxy radical
Oxidation of Met35
Stabilization of Met radical
D23
E22
COO•
Aggregation
Dimer
Trimer
D23 E22
Toxic oligomers
2 x n-mer
3 x n-mer

Figure 4

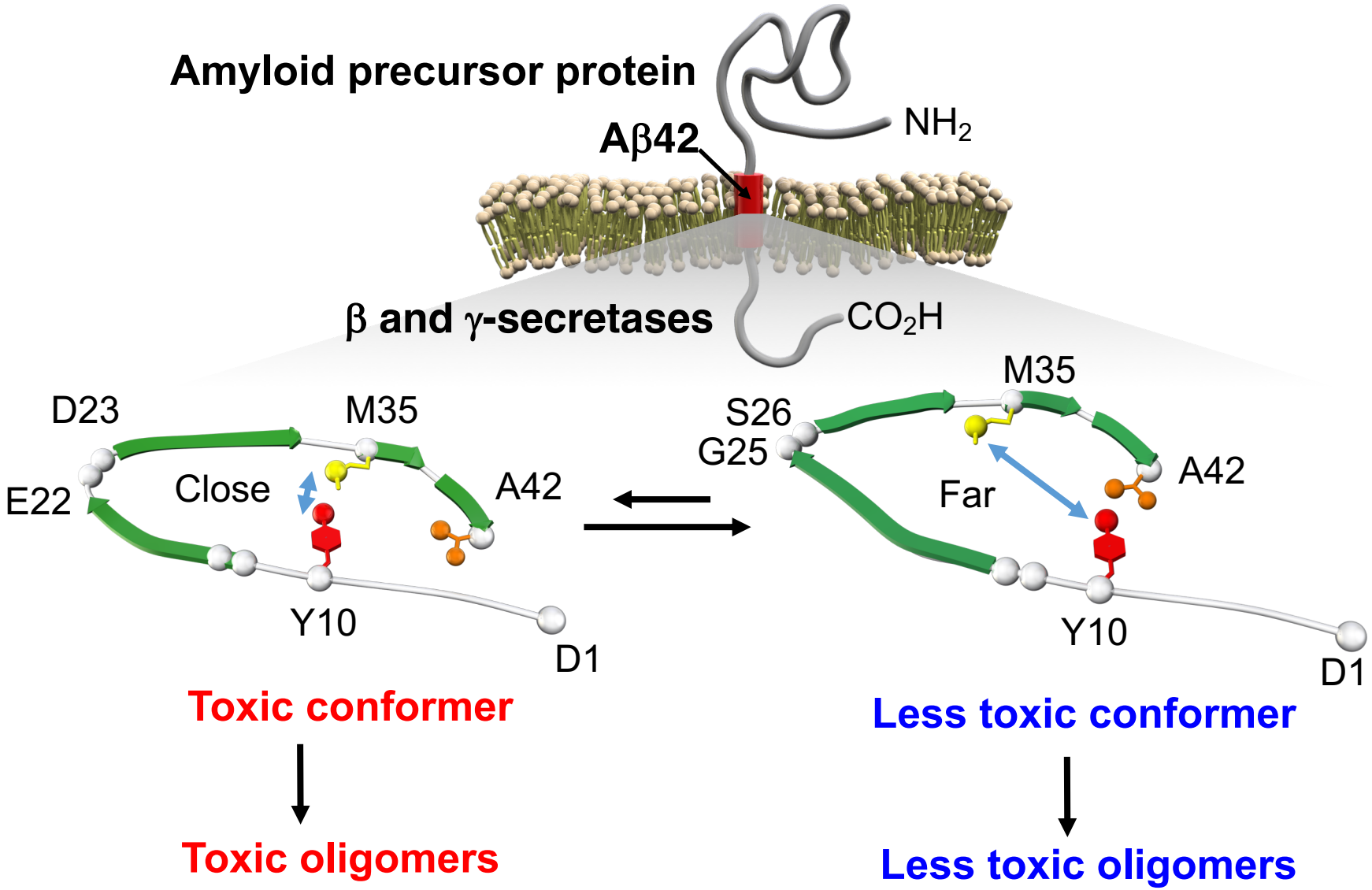
Amyloid precursor protein
Aβ42
NH2
β and γ-secretases
CO2H
D23
M35
E22
Close
A42
Y10
D1
Toxic conformer
Toxic oligomers
S26
G25
M35
Far
A42
Y10
D1
Less toxic conformer
Less toxic oligomers

Figure 5

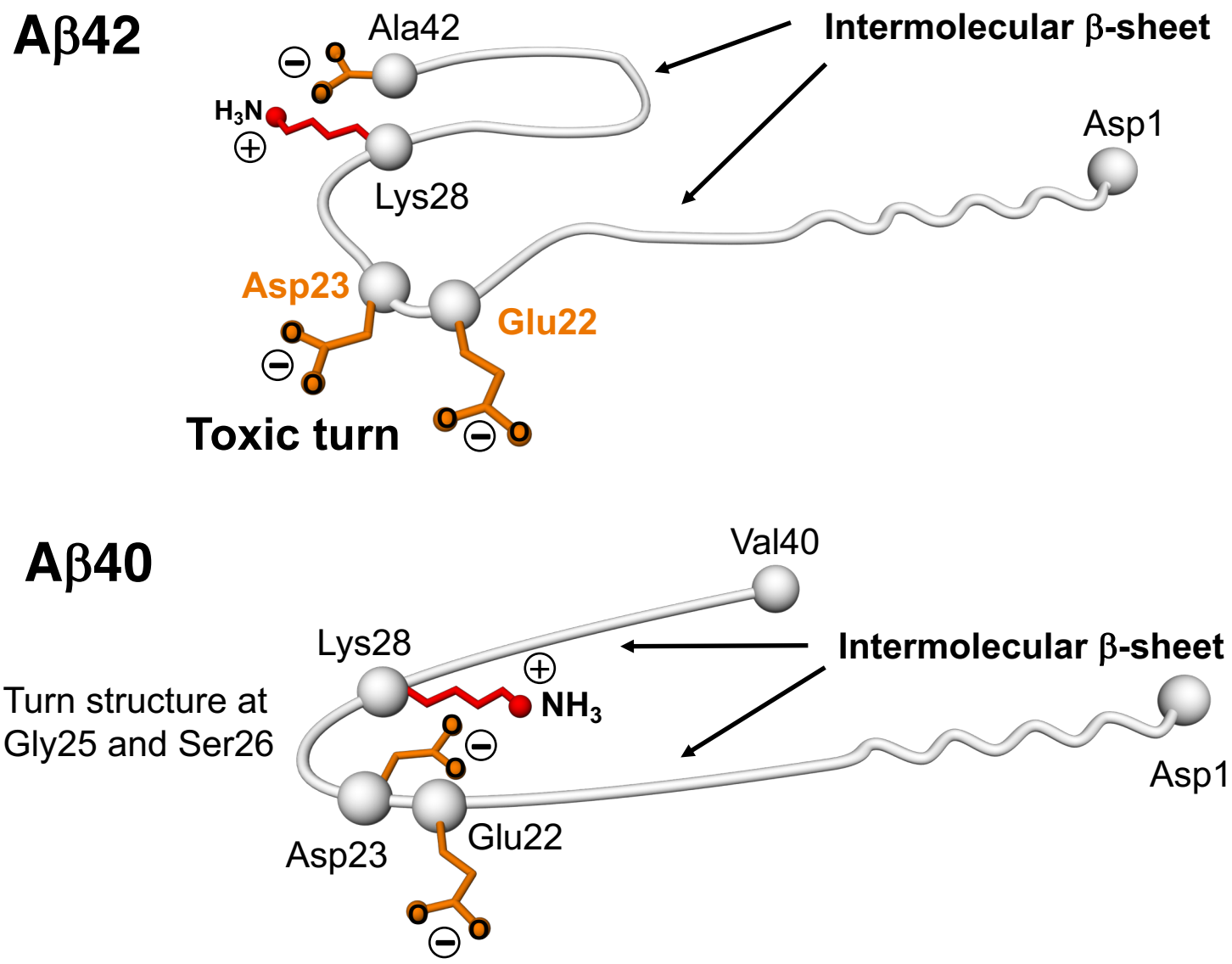
Aβ42
Ala42
Intermolecular β-sheet
H3N
Asp1
Lys28
Asp23
Glu22
Toxic turn
Aβ40
Val40
Lys28
Intermolecular β-sheet
Turn structure at
Gly25 and Ser26
NH3
Asp1
Asp23
Glu22

Figure 6

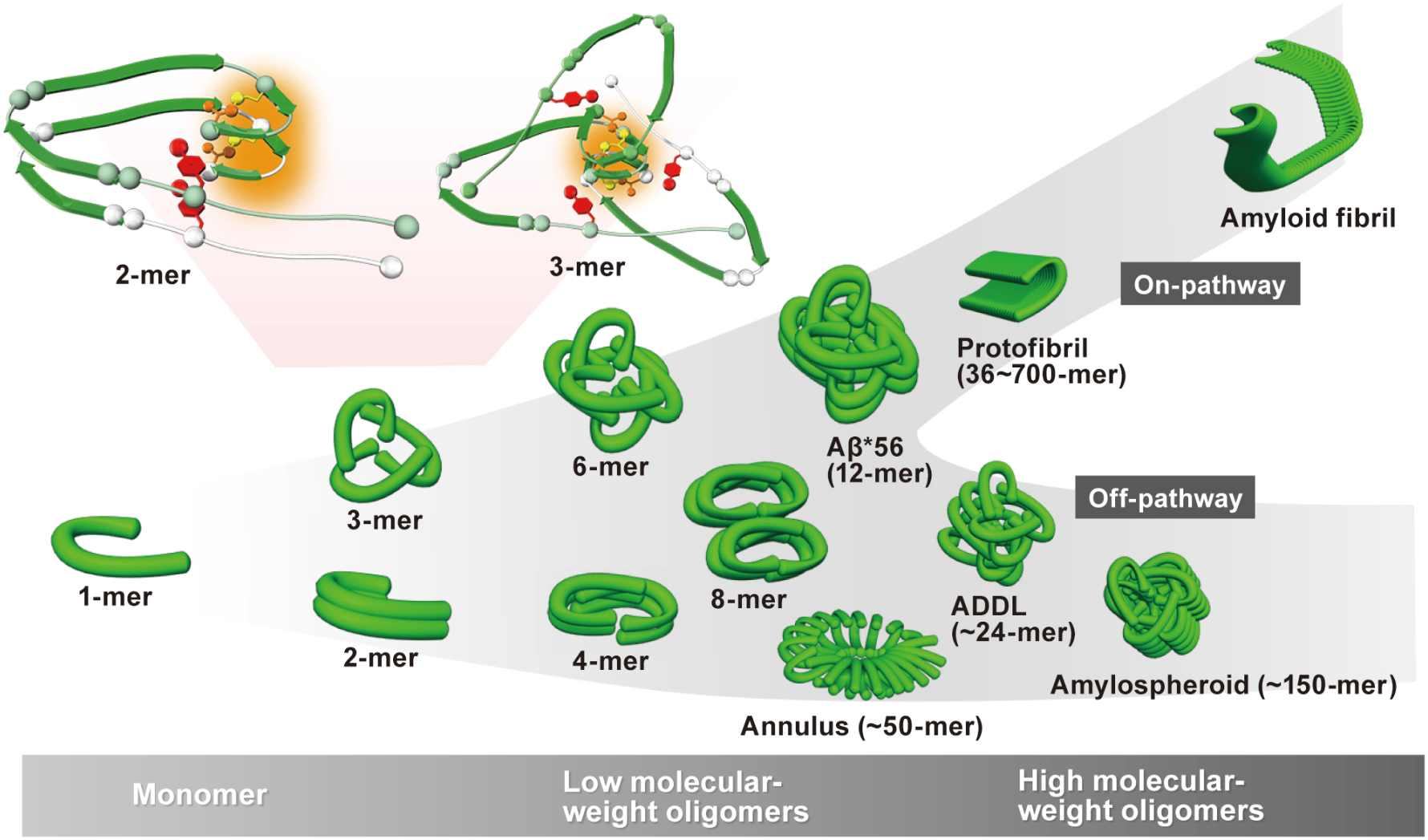
2-mer
3-mer
Amyloid fibril
On-pathway
Protofibril
(36~700-mer)
6-mer
Aβ*56
(12-mer)
3-mer
Off-pathway
1-mer
8-mer
ADDL
(~24-mer)
2-mer
4-mer
Amylospheroid (~150-mer)
Annulus (~50-mer)
Monomer
Low molecular-weight oligomers
High molecular-weight oligomers

Figure 7

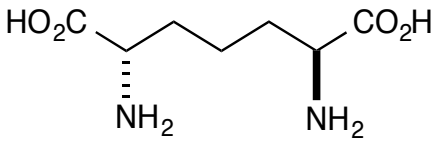

L,L-Diaminopimelic acid (DAP)

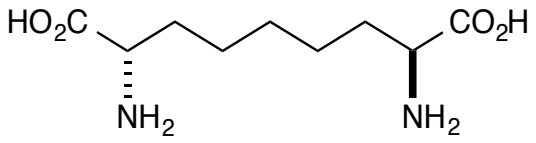

L,L-Diaminoazelaic acid (DAZ)

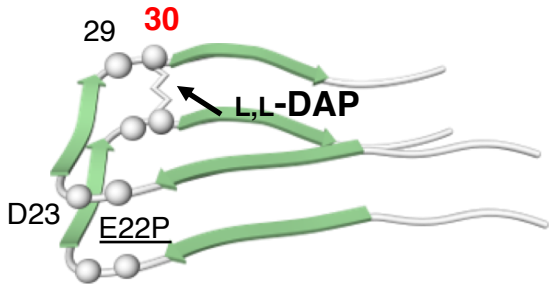

E22P,A30DAP-Aβ40 dimer (**1**)

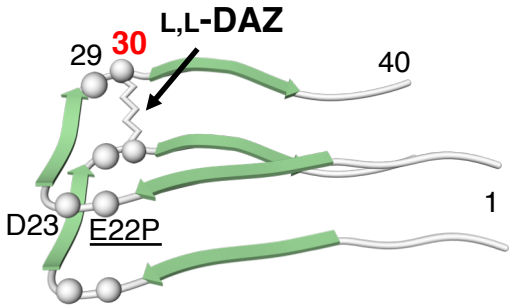

E22P,A30DAZ-Aβ40 dimer (**2**)

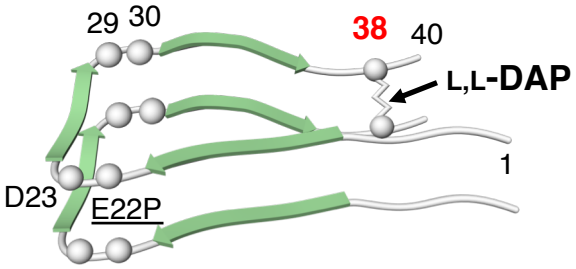

E22P,G38DAP-Aβ40 dimer (**3**)

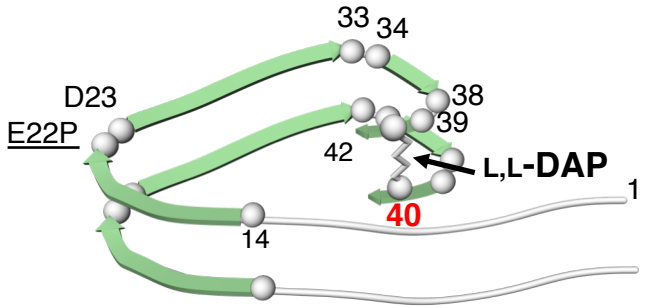

E22P,V40DAP-Aβ42 dimer (**4**)

Figure 8

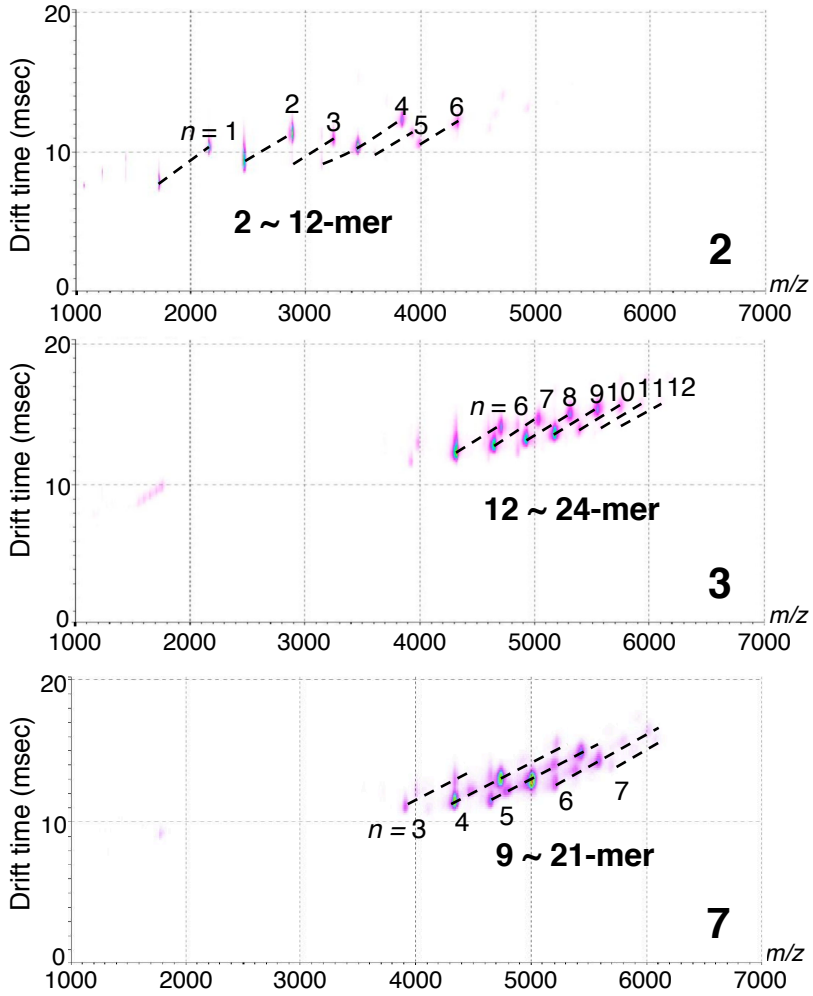
Drift time (msec)
m/z
n = 1
2
3
4
5
6
2 ~ 12-mer
2
n = 6
7
8
9
10
11
12
12 ~ 24-mer
3
n = 3
4
5
6
7
9 ~ 21-mer
7

Figure 9

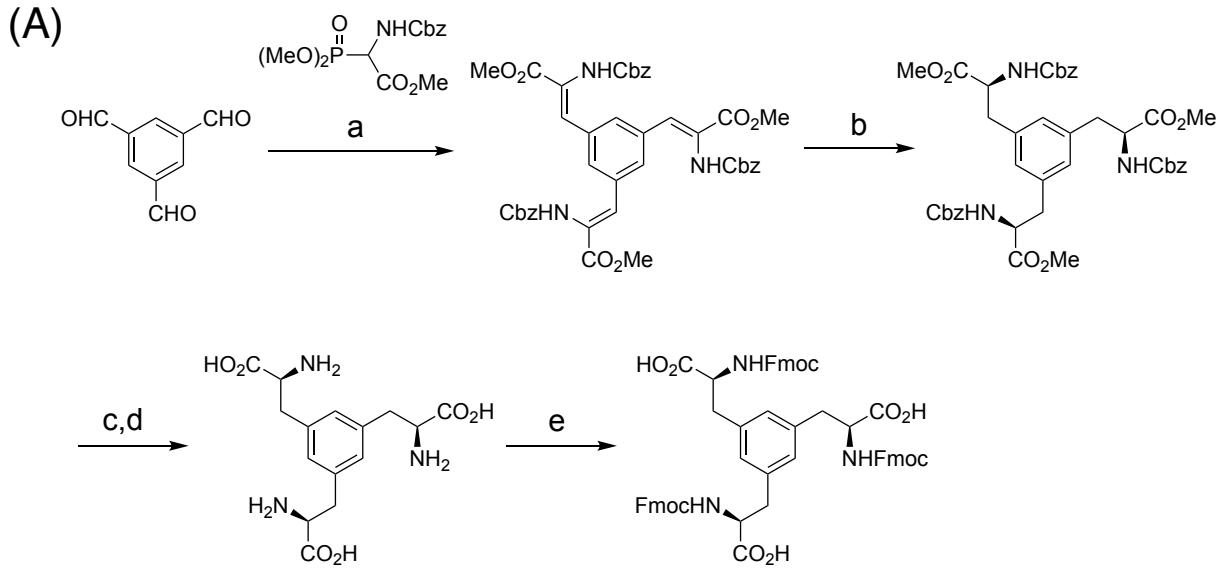

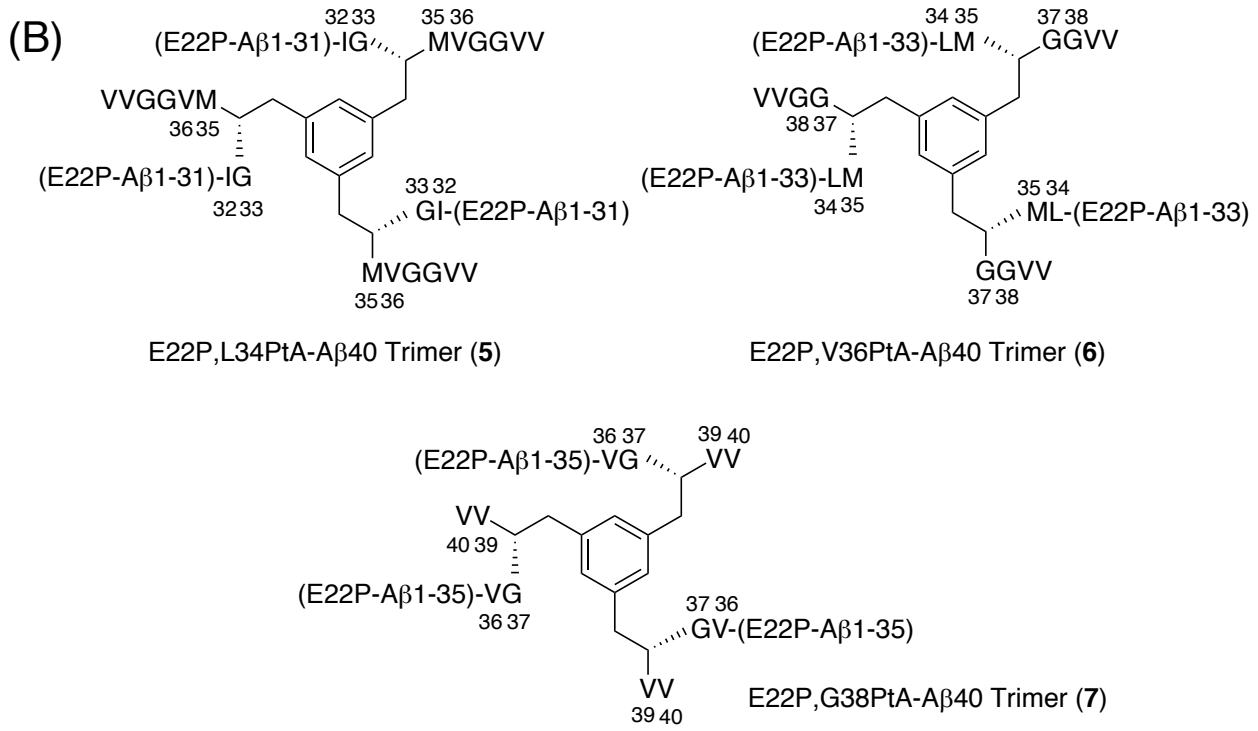

E22P,L34PtA-Aβ40 Trimer (**5**)

E22P,V36PtA-Aβ40 Trimer (**6**)

E22P,G38PtA-Aβ40 Trimer (**7**)

Figure 10

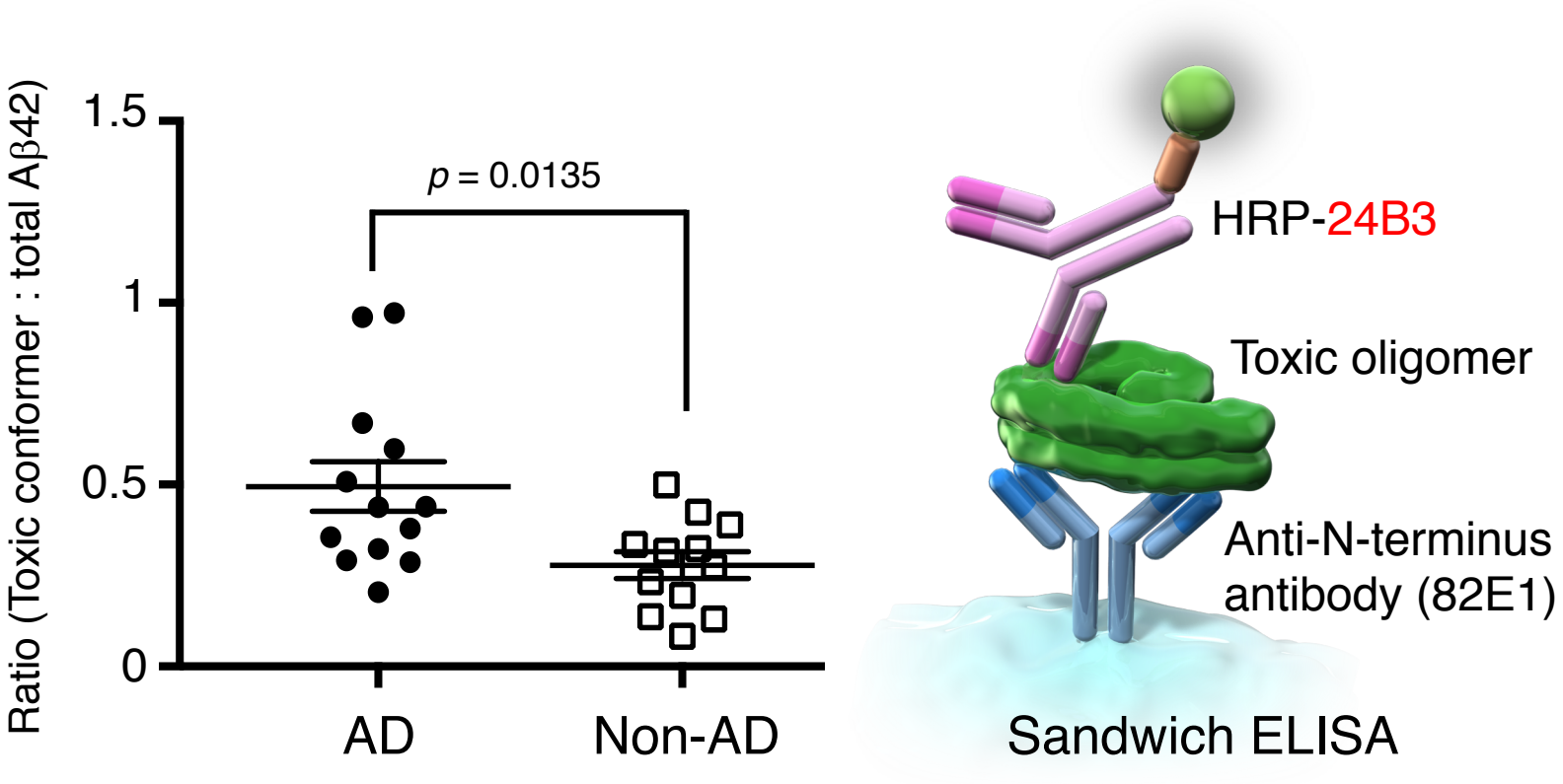
Ratio (Toxic conformer : total Aβ42)
1.5
1
0.5
0
p = 0.0135
AD
Non-AD
HRP-24B3
Toxic oligomer
Anti-N-terminus antibody (82E1)
Sandwich ELISA

Figure 11

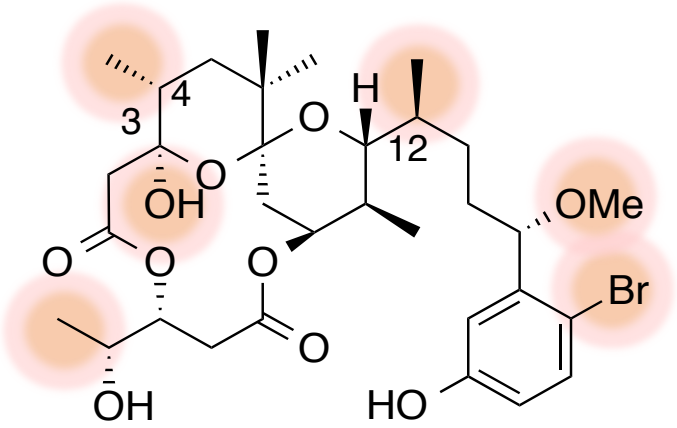

Extraction of anti-proliferative activity

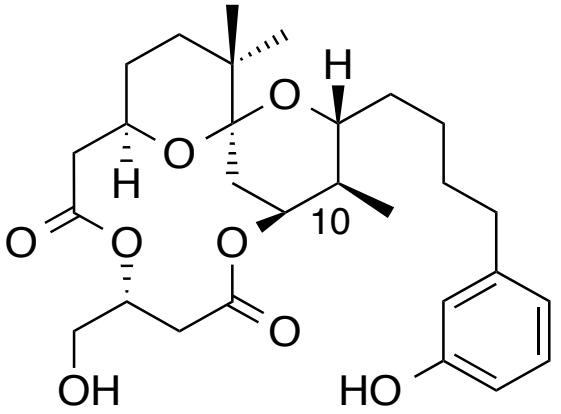

“Master key”

Aplysiatoxin (ATX)

Tumor promoting
Proinflammatory

Potent PKC ligand
Anti-proliferative activity

High toxicity *in vivo*

“Special key”

10-Me-aplog-1

Non-tumor promoting
Non-proinflammatory

Potent PKC ligand
Anti-proliferative activity

Low toxicity *in vivo*

Figure 12